minerals

MDPI

Article

Rüdlingerite, $Mn^{2+}_2V^{5+}As^{5+}O_7{\cdot}2H_2O$, a New Species Isostructural with Fianelite

Philippe Roth [1,*], Nicolas Meisser [2], Fabrizio Nestola [3], Radek Škoda [4], Fernando Cámara [5], Ferdinando Bosi [6,7], Marco E. Ciriotti [8,9], Ulf Hålenius [10], Cédric Schnyder [2,11] and Roberto Bracco [12]

1 Swiss Seismological Service, ETH Zürich, 8092 Zurich, Switzerland
2 Musée cantonal de géologie, Université de Lausanne, 1015 Lausanne, Switzerland; nicolas.meisser@unil.ch
3 Dipartimento di Geoscienze, Università degli studi di Padova, 35131 Padova, Italy; fabrizio.nestola@unipd.it
4 Department of Geological Sciences, Masaryk University, 611 37 Brno, Czech Republic; rskoda@sci.muni.cz
5 Dipartimento di Scienze della Terra, Università degli Studi di Milano, 20133 Milano, Italy; fernando.camara@unimi.it
6 Dipartimento di Scienze della Terra, Sapienza Università di Roma, 00185 Rome, Italy; ferdinando.bosi@uniroma1.it
7 CNR–Istituto di Geoscienze e Georisorse, UOS Roma, 00185 Roma, Italy
8 Dipartimento di Scienze della Terra, Università degli Studi di Torino, 10125 Torino, Italy; marco.ciriotti@unito.it
9 Associazione Micromineralogica Italiana, 10073 Devesi-Cirié, Italy
10 Department of Geosciences, Swedish Museum of Natural History, 10405 Stockholm, Sweden; ulf.halenius@nrm.se
11 Secteur des Sciences de la Terre, Muséum d'histoire naturelle, 1208 Genève, Switzerland; cedric.schnyder@ville-ge.ch
12 Associazione Micromineralogica Italiana, 17100 Savona, Italy; woof_59@yahoo.it
* Correspondence:philippe.roth@sed.ethz.ch

Received: 17 September 2020; Accepted: 22 October 2020; Published: 27 October 2020

Abstract: The new mineral species rüdlingerite, ideally $Mn^{2+}_2V^{5+}As^{5+}O_7{\cdot}2H_2O$, occurs in the Fianel mine, in Val Ferrera, Grisons, Switzerland, a small Alpine metamorphic Mn deposit. It is associated with ansermetite and Fe oxyhydroxide in thin fractures in Triassic dolomitic marbles. Rüdlingerite was also found in specimens recovered from the dump of the Valletta mine, Canosio, Cuneo, Piedmont, Italy, where it occurs together with massive braccoite and several other As- and V-rich phases in richly mineralized veins crossing the quartz-hematite ore. The new mineral displays at both localities yellow to orange, flattened elongated prismatic, euhedral crystals measuring up to 300 μm in length. Electron-microprobe analysis of rüdlingerite from Fianel gave (in wt%): MnO 36.84, FeO 0.06, As_2O_5, 25.32, V_2O_5 28.05, SiO_2 0.13, H_2O_{calc} 9.51, total 99.91. On the basis of 9 O anions per formula unit, the chemical formula of rüdlingerite is $Mn_{1.97}(V^{5+}_{1.17}As_{0.83}Si_{0.01})_{\Sigma 2.01}O_7{\cdot}2H_2O$. The main diffraction lines are [d_{obs} in Å (I_{obs}) hkl]: 3.048 (100) 022, 5.34 (80) 120, 2.730 (60) 231, 2.206 (60) 16-1, 7.28 (50) 020, 2.344 (50) 250, 6.88 (40) 110, and 2.452 (40) 320. Study of the crystal structure showcases a monoclinic unit cell, space group $P2_1/n$, with a = 7.8289(2) Å, b = 14.5673(4) Å, c = 6.7011(2) Å, β = 93.773(2)°, V = 762.58(4) Å^3, Z = 4. The crystal structure has been solved and refined to R_1 = 0.041 on the basis of 3784 reflections with $F_o > 4\sigma(F)$. It shows Mn^{2+} hosted in chains of octahedra that are subparallel to [-101] and bound together by pairs of tetrahedra hosted by V^{5+} and As^{5+}, building up a framework. Additional linkage is provided by hydrogen-bonding through H_2O coordinating Mn^{2+} at the octahedra. One tetrahedrally coordinated site is dominated by V^{5+}, $^{T(1)}(V_{0.88}As_{0.12})$, corresponding to an observed site scattering of 24.20 electrons per site (eps), whereas the second site is strongly dominated by As^{5+}, $^{T(2)}(As_{0.74}V_{0.26})$, with, accordingly, a higher observed site scattering of 30.40 eps. The new mineral has been approved by the IMA-CNMNC and named for Gottfried Rüdlinger (born 1919), a pioneer in the 1960–1980s, in the search and study of the small minerals from the Alpine manganese mineral deposits of Grisons.

Keywords: rüdlingerite; new mineral species; fianelite; vanadium; arsenic; crystal structure; Fianel mine; Switzerland; Valletta mine; Italy

1. Introduction

In 1996, Brugger and Berlepsch (1996) [1] described fianelite, the then only second Mn vanadate and the first new mineral species for the Fianel mine, where the exotic mineral association was summarily sensed by Stucky (1960) [2]. Later, two new Mn species, ansermetite [3] and scheuchzerite [4], followed. In their description of fianelite, $Mn_2V_2O_7 \cdot 2H_2O$, Brugger and Berlepsch (1996) [1] noticed that substitution of As for V occurs on the second tetrahedrally coordinated V site and that As could potentially even dominate in this site. The IMA-CNMNC dominant-constituent rule [5–7] generally states that in order for a mineral to be a distinct species: "*At least one structural site in the potential new mineral should be predominantly occupied by a different chemical component than that which occurs in the equivalent site in an existing mineral species"*. The dominant-constituent rule is applied in most approved new-mineral proposals but in complex systems, like e.g., the epidote group, "*the dominant-constituent rule has been extended by considering "a group of atoms with the same valency state" as a single constituent"* [6,7]. During a systematic energy-dispersive X-ray spectroscopy (EDXS) screening of fianelite material from the Fianel mine, a specimen turned out to be abnormally As-rich, pointing to the possible existence of a new mineral species.

During the work related to the project "Characterization of new and rare mineral species" started in 2010 by the Italian Micromineralogical Association (AMI) and carried out through EDXS and microRaman complementary spectroscopies, a particular sample from Fianel (R.B. collection) was identified in which bright yellow crystals were associated with bright red crystals. The Raman spectrum of the red mineral (fianelite) turned out to be rather different from the analogous spectrum of the yellow mineral (now rüdlingerite). At the same period, studies were underway on a lot of specimens from the recently discovered Valletta mine. In some of them, the mineralogical association appeared to be the same and consequently the yellow and red Valletta crystals were also analysed (co-type specimen), leading to the discovery that the EDXS and Raman analytical responses were the same as their Fianel counterparts.

The As-rich mineral was shown to have an As dominance on the second tetrahedrally coordinated site. Sticking to the general dominant-constituent rule and thereby considering that the homovalent substitution encountered at the two tetrahedrally coordinated sites in this phase is not a complex system, the new mineral and its name, rüdlingerite, were submitted to and accepted by the Commission on New Minerals, Nomenclature and Classification (CNMNC) of the International Mineralogical Association (IMA) (proposal # 2016-054a). The description is based primarily upon one holotype and one cotype specimen. The holotype from the Fianel mine is deposited in the Mineralogical Collection of the Musée cantonal de géologie, University of Lausanne, Anthropole-Dorigny, CH-1015 Lausanne, Switzerland, catalogue number MGL N° 080116. A cotype from the Valletta mine is deposited in the Mineralogical Collection of the Dipartimento di Scienze della Terra of the Università di Torino stored in the Museo Regionale di Scienze Naturali di Torino, Sezione di Mineralogia, Petrografia e Geologia, via Giovanni Giolitti 36, I-10123 Torino, Italy, catalogue number M/U 17121.

The name rüdlingerite honors Gottfried Rüdlinger (born 1919), a private collector and pioneer in the 1960–1980s who engaged in the search and study of the small minerals from the Alpine manganese mineral deposits of Grisons. G. Rüdlinger was long-time president of the local section of the Swiss association of 'strahlers' and mineral collectors and designed the mineral exhibit at the Nature Museum in Chur [8].

2. Occurrence

2.1. Holotype

Rüdlingerite was found in a specimen labeled as "fianelite", originally from the Fianel mine in Val Ferrera, Grisons, Switzerland (46°32′47′′ N, 9°27′43′′ E). The Fianel deposit is a lenticular ore body within the Triassic dolomitic marbles that are part of the Mesozoic cover of the Suretta nappe, a member of the paleogeographic "Briançonnais" domain. The deposit underwent several phases of Alpine metamorphism with a climax at conditions of the blueschist to greenschist-facies [9]. Fianel is remarkable for the diversity of its ore types and consequently of its mineralogy. One type of ore consists of stratabound, medaite-rich, up to 20 cm thick and 2 m long lenses, crosscut by several generations of cm-wide veinlets [1]. These veins are themselves crosscut by thin fractures containing fianelite, rüdlingerite, ansermetite, and Fe oxyhydroxide. Fianelite, rüdlingerite, and ansermetite represent the last stage in the remobilization of V and As [1]. On the specimens investigated, rüdlingerite occurs as light orange, slightly flattened, prismatic crystals up to 300 μm in length. They are associated with anhedral ansermetite.

2.2. Cotype

Rüdlingerite was also found on specimens recovered from the dump of the Valletta mine, Canosio, Piedmont, Italy (44°23′42′′ N, 7°5′42′′ E). The Valletta mine is a small Fe-Mn deposit that has not been worked in modern times and has never been studied geologically or petrologically. The geological setting is rather similar to that of the Fianel mine and has been summarized by Cámara et al. (2014) [10] in their description of the new mineral grandaite, for which, with braccoite [11], canosioite [12], castellaroite [13], lombardoite [14], and piccoliite[15], the Valletta mine is also the type locality.

At the Valletta mine, rüdlingerite is a secondary mineral crystallized from hydrothermal fluids in an oxidizing environment. It was found in richly mineralized veins crossing the quartz-hematite ore. The main mineralization is made up of extended, massive braccoite veins and millimeter-sized grains having manganberzeliite/palenzonaite composition at the core and berzeliite on the rim. Other As- and V- rich phases (adelite, arseniopleite, canosioite, castellaroite, coralloite, bariopharmacosiderite, berzeliite, gamagarite, grandaite, palenzonaite, pyrobelonite, saneroite, tilasite, tiragalloite, tokyoite, wallkilldellite, some brackebuschite group arsenates currently under study, and other not yet well characterized As- and V-bearing minerals) are also present at the locality.

Like at the Fianel mine, the very rare open fractures host late phases that have developed euhedral crystals: rüdlingerite as yellow to light yellow-orange, flattened, elongated prismatic crystals measuring up to 200 μm in length, and fianelite as smaller, less elongated, deep red crystals closely resembling those from the Swiss type locality. Depending on local conditions, either species can be dominant in a single specimen. Rare radiating aggregates of bronze-brown wallkilldellite have also been observed.

3. Appearance and Physical Properties

At the Fianel mine, rüdlingerite occurs as light orange, prismatic crystals that reach 300 μm in length (Figure 1). At the Valletta mine, the new mineral occurs as yellow to light yellow-orange, flattened, elongated prismatic crystals measuring up to 200 μm length, associated with fianelite as smaller, less elongated, deep red crystals (Figure 2) closely resembling those from the Swiss type locality. Crystal forms were not determined but on the basis of SEM observations and photos, the dominant forms can be assigned to the pinacoid {010} and the prisms {110}, {041} and {011}, in agreement with the crystal habit and forms of fianelite, goniometrically determined by Brugger and Berlepsch (1996) [1]. Accordingly, crystal elongation is parallel [001]. Twinning has not been observed.

Rüdlingerite is transparent to translucent, has a vitreous luster, and a yellowish-white streak. It is non-fluorescent. Mohs hardness has been determined through scratch tests and found to be 3½.

Rüdlingerite is brittle, with a perfect cleavage on {001} and a curved fracture. Parting was not observed. The density could be determined by floatation of a Fianel sample in diiodomethane–1–chloronaphtalene system (23° C) and was found to be 3.28(2) g·cm^{-3}. Based on the empirical formulae, the calculated densities are 3.298 g·cm^{-3} for the Fianel sample and 3.322 g·cm^{-3} for the Valletta sample.

Optically, rüdlingerite is biaxial (sign unknown) and $2V_{meas.}$ is smaller than 10°. The average refractive index calculated using the Gladstone-Dale relationship is $1.791 < n_{av} < 1.799$ for the average composition of the Fianel material. The refractive index n_{av}, measured using immersion method in refractive index liquid in the diodomethane–tin tetrabromide–sulphur system (CH_2I_2–SnI_4–S; $1.78 < n < 1.82$) [16] and verified using a Leitz-Jelley microrefractometer [17] is $n_{av} \geq 1.80$ (589 nm). The high chemical reactivity of index liquid, due to the hydrolysis toward hydrated minerals, precludes complete data measurements. After several minutes of immersion, rüdlingerite crystals are destroyed. The flattened prismatic habitus of rudlingerite, with resulting small particle dimensions perpendicular to Z, precluded observations of bisectrix-centered interference figures of required quality. Rüdlingerite shows a strong pleochroism from yellow to orange; it displays positive elongation; $Z \wedge c \sim 14°$. For the Valletta specimen, X = yellow, Y = orange yellow, Z = brownish orange; $X < Y << Z$.

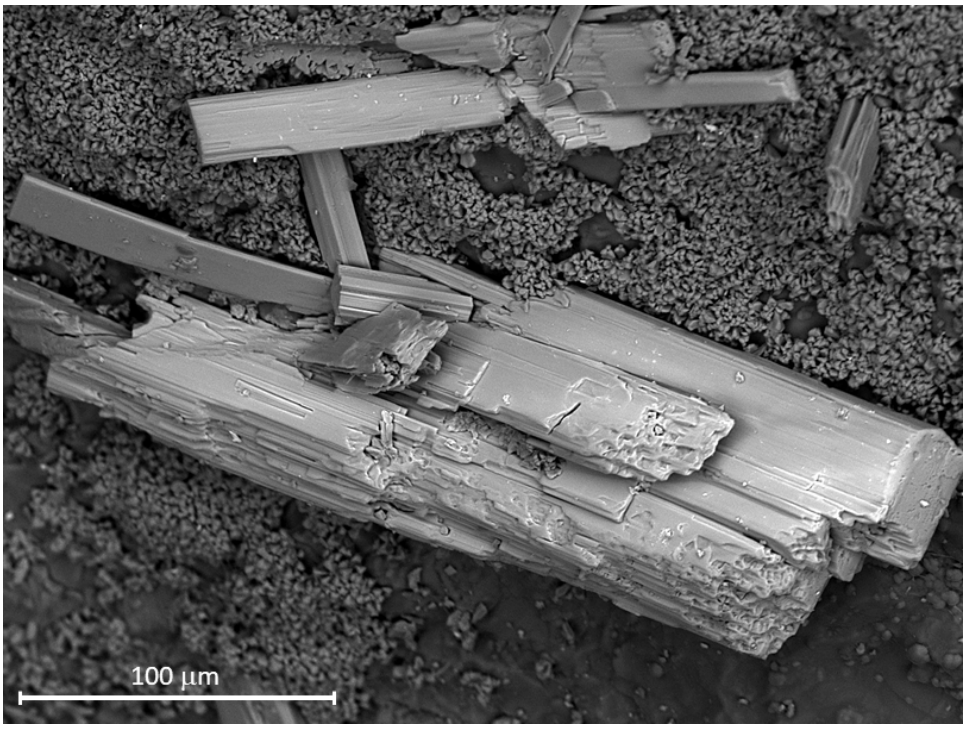

Figure 1. Scanning Electronic Microscope (SEM) image of rüdlingerite crystals from Fianel.

Figure 2. Yellow to orange platy crystals of rüdlingerite (0.1 mm long) with dark orange to red fianelite crystals from Valletta (R. Bracco photo).

4. Chemical Data

The results of the chemical analyses are summarized in Table 1. Chemical compositions of the Fianel and Valletta specimens were obtained by electron microprobe techniques (WDS mode) using 16 point analyses performed with the use of a Cameca SX100 instrument (located at the Department of Geological Sciences in Brno, Czech Republic, and operated at 15 kV, 10 nA at a beam diameter of 8 µm) and 4-point analyses performed with a Cameca SX50 instrument (located at the Department of Earth Sciences, Sapienza University, Rome, Italy, and operated at 15 kV, 15 nA at a beam diameter of 1 µm), respectively. The standards used are given in Table 1. Other possible or likely elements were sought by WDS, but found to be below the detection limits.

Table 1. Chemical composition (wt%) of rüdlingerite from Fianel and Valletta Mines.

Constituent	Fianel Specimen (16 Point Analyses)			Valletta Specimen (4 Point Analyses)			Standard Fianel/Valletta
	Mean	Range	SD	Mean	Range	SD	
CaO	b.d.l.			0.04	0.01–0.06	0.02	Wollastonite
MnO	36.84	36.41–37.21	0.72	35.25	34.79–35.66	0.40	Rhodonite
FeO	0.06	0.00–0.12	0.07	b.d.l.			Almandine
ZnO	b.d.l.			0.03	0.00–0.05	0.02	ZnO/Zn
As_2O_5	25.32	23.23–28.59	0.64	27.59	26.65–29.23	1.13	Lammerite/ synth. GaAs
V_2O_5	28.05	25.34–30.25	0.20	26.47*	24.06–28.36	1.80	Synth. $ScVO_4$/ vanadinite
SiO_2	0.13	0.00–0.21	0.04	b.d.l.			Sanidine
H_2O**	9.51			9.25			
Total	99.91			98.34*			

b.d.l. = below detection limit. *An amount of V_2O_3 = 1.35 wt% has been calculated on the basis of V^{3+} at the *Mn*(1,2) sites as suggested by an initial, tentative structure refinement of the Valletta sample; therefore the amount of V_2O_5 has to be reduced to 24.83 wt%. **Calculated on the basis of charge balance, required (OH) *pfu* to charge compensate for V^{3+} at the *Mn*(1,2) sites and O = 9 *apfu*.

Raw X-ray intensities were corrected for matrix effects with a ϕ(ρz) algorithm of X-PHI routine [18]. Because insufficient material was available for a direct determination of H_2O, the amount of water was calculated on the basis of charge balance and O = 9 *apfu*, as determined by the crystal structure analysis.

The empirical formulae calculated on the basis of 9 O apfu are:

- For Fianel: $Mn_{1.97}{}^{T(1)+T(2)}(V^{5+}{}_{1.17}As_{0.83}Si_{0.01})_{\Sigma 2.01}O_{7.00}\cdot 2H_2O$
- For Valletta: $(Mn_{1.93}V^{3+}{}_{0.07})_{\Sigma 2.00}{}^{T(1)+T(2)}(V^{5+}{}_{1.06}As_{0.93})_{\Sigma 1.99}[O_{6.98}(OH)_{0.02}]_{\Sigma 7.00}\cdot 1.98H_2O$

The ideal formula is $Mn_2{}^{T(1)}V^{5+}{}^{T(2)}As^{5+}O_7 \cdot 2H_2O$, which requires As_2O_5 31.25, V_2O_5 20.38, MnO 38.58, H_2O 9.79, total 100 wt%.

Chemical tests have shown rüdlingerite to be insoluble in H_2O and slightly soluble in dilute (10%) HCl at room temperature.

5. Raman Spectroscopy

A Raman spectrum of rüdlingerite from Fianel mine was obtained with a Leica DM 2500 microscope, equipped with 5×, 10×, 20×, 50×, and 100× objectives and part of a Renishaw inVia spectrometer, which includes a monochromator, a filter system, and a Charge Coupled Device (CCD), located in the Natural History Museum of Geneva, Geneva, Switzerland. The Raman spectrum was obtained by a He-Ne Laser (633 nm) at a nominal resolution of 2 cm^{-1} in the range 100–4000 cm^{-1}. A power of 1.7 mW on the sample was set, during a time of 10 s for a single analysis. The analysis was conducted on a single prismatic crystal, with the laser beam orthogonal to the elongation direction of the crystal. The representative spectrum is shown in Figure 3.

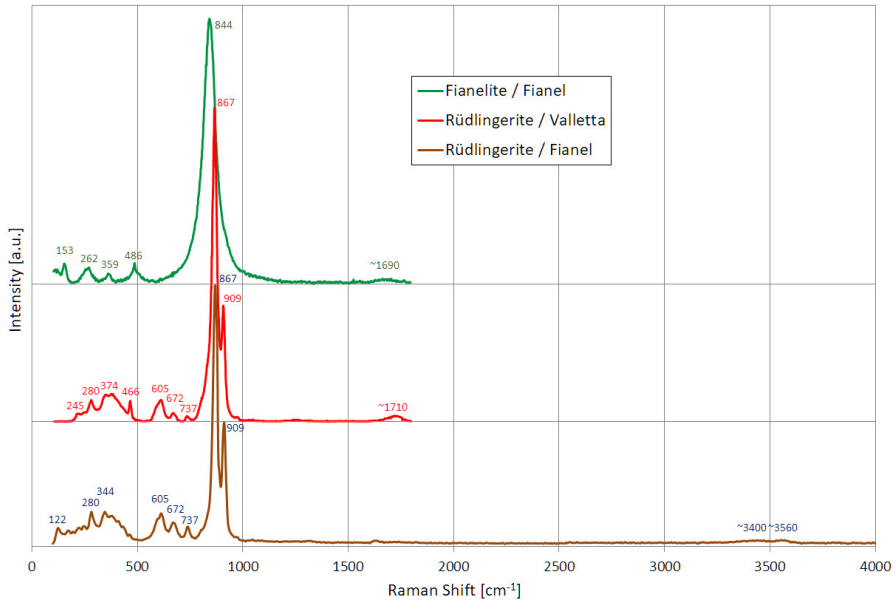

Figure 3. Comparison of the microRaman spectra of rüdlingerite and of fianelite from Fianel and of rüdlingerite from Valletta. The differences between the rüdlingerite spectra and the fianelite spectrum are evident in the range 600–1000 cm^{-1}.

Raman spectra of rüdlingerite from the Valletta mine and of fianelite from the Fianel mine (see Figure 3) were acquired using a micro/macro Jobin Yvon Mod. LabRam HRVIS, equipped with a motorized x-y stage and an Olympus microscope and located at the Department of Earth Sciences, Torino University, Torino, Italy. The backscattered Raman signal was collected with 20× objective and the Raman spectrum was obtained for a non-oriented single crystal. The 532 nm line of a Nd:YAG laser was used as excitation; laser power (80 mW) was controlled by means of a series of density filters. The minimum lateral and depth resolution was set to few μm. The system was calibrated using the 520.6 cm^{-1} Raman band of silicon before each experimental session. The spectra were collected with multiple acquisitions (2 to 4) with single counting times ranging between 50 and 100 s. Spectral manipulation such as baseline adjustment, smoothing and normalization were performed using the

Labspec 5 software package [19]. After background removal, band component analysis was undertaken using the Fityk software package [20], assuming combined Lorentzian-Gaussian band shapes and applying Voigt function.

The presence of $(AsO_4)^{3-}$ is confirmed in both samples, but it is very difficult to separate the contributions of arsenate from those of vanadate units as the bands of the two units partly overlap each other (e.g., [21]). In the region 100–600 cm^{-1} multiple Raman bands are observed at 122 (Fianel), 245 (Valletta), 280 (both) (all corresponding to lattice modes, according to Frost et al., 2009 [22]), 344 (Fianel), and 374 (Valletta) cm^{-1} (As^{5+}–O symmetric bending vibrations [23]). A weak and sharp band centred around 466 cm^{-1} is also present in the Valletta spectrum. In the region of 600–800 cm^{-1}, weak, multiple overlapping bands are observed at 605, 672, and 737 cm^{-1} in the spectra of both localities. The former two bands are assigned to the assumed OH vibration modes, while the latter is thought to be related to the As–metal-oxygen bonds. The most intense bands are centred at 867 and 909 cm^{-1}, corresponding to $(AsO_4)^{3-}$ and $(VO_4)^{3-}$ symmetric stretching nodes [22,24,25]. The splitting of this main peak may be attributable to As occupying both *T* sites in rüdlingerite, but only *T*(2) in fianelite. The flattened band at ~1710 cm^{-1} in the Valletta spectrum could be assigned to δH_2O bending mode of hydrogen bonded water molecules. Two weak and broad bands in the region 3300–3600 cm^{-1} of the Fianel spectrum are attributable to O–H stretching modes of the H_2O groups [22].

6. Crystallography and Crystal Structure

Rüdlingerite is monoclinic, space group $P2_1/n$. Powder X-ray diffraction (PXRD) data for rüdlingerite from Fianel were collected using a 114.6 mm diameter Gandolfi Camera (Ni-filtered Cu$K\alpha$ radiation and Si as internal standard) located at the Musée cantonal de géologie, Lausanne. The LATCON program [26] was used to refine the PXRD data after light correction using Si as internal standard. The results are summarized in Table 2. The unit cell parameters calculated from the powder data are as follows: a = 7.814(7) Å, b = 14.63(1) Å, c = 6.690(6) Å, β = 93.63(6)°, V = 764(2) $Å^3$ and Z = 4.

Table 2. X-ray powder diffraction data for rüdlingerite from Fianel. The strongest diffraction lines are given in bold.

d_{obs}[Å]	d_{calc}[Å]	I_{obs}*	*hkl*
7.28	7.31	50	020
6.88	6.89	40	110
6.07	6.08	30	011
5.34	5.34	80	120
4.93	4.97	10	021
4.68	4.70	20	111
4.12	4.14	20	130
3.943	3.939	20	031
3.453	3.443	30	220
3.249	3.258	30	012
3.048	3.039	100	022
2.776	3.793	30	122
2.730	2.736	60	231
2.618	2.631	40	13-2
2.557	2.558	30	21-2
2.452	2.451	40	320
2.344	2.341	50	250
2.206	2.207	60	16-1
1.969	1.999	10	341
1.836	1.850	40	351
1.833	1.832	40	143

* Intensities may be affected by preferred orientation.

Single-crystal X-ray studies were carried out on the Fianel holotype using a Rigaku-Oxford Diffraction Supernova diffractometer installed at the Department of Geosciences, University of Padova, Italy, equipped with a 200K Pilatus Dectris detector and with a micro-source with Mo$K\alpha$ radiation (λ = 0.71073 Å); the detector-to-crystal distance was 68 mm. They confirmed the space group and delivered the following data: a = 7.8289(2) Å, b = 14.5673(4) Å, c = 6.7011(2) Å, β = 93.773(2)°, V = 762.58(4) Å^3 and Z = 4.

Single crystal data were also obtained for a cotype specimen from Valletta using an Oxford Gemini R Ultra diffractometer equipped with a CCD area detector and graphite-monochromatized Mo$K\alpha$ radiation (λ = 0.71073 Å) installed at Centro Interdipartimentale di Ricerca per lo Sviluppo della Cristallografia Diffrattometrica-CRISDI, Torino University, Torino, Italy. The space group was confirmed, and the following unit cell parameters were obtained: a = 7.8278(3) Å, b = 14.5739(7) Å, c = 6.6962(3) Å, β = 93.820(4)°, V = 762.22(6) Å^3, Z = 4.

The a:b:c ratios calculated from the unit-cell parameters are (single-crystal data) 0.5374:1:0.4600 for Fianel and 0.5371:1:0.4595 for Valletta.

Complete diffraction intensity data collection allowed refining the structure of the Fianel holotype and Valletta cotype starting from the atom coordinates of Brugger and Berlepsch (1996) [1]. The crystal structure was refined to R_1 = 0.041–0.046 by means of the SHELX-2018 package [27] on the basis of 3784–2027 independent reflections with $F_o > 4\sigma(F)$. Experimental results are reported in Table 3. The crystal structure refinement of rüdlingerite provides results very close to those of fianelite. The coordinates of H atoms were located in the Fourier difference map and added to the refinement soft restraints of 0.96(2) Å on the O–H distances, and with the U_{iso} of each H set to ×1.2 that of its donor O atom.

Table 3. Crystal Data and Structure Refinement for Rüdlingerite Holotype from the Fianel Mine and Cotype from the Valletta Mine.

Identification Code	Fianel	Valletta
Formula weight	378.05	373.67
Wavelength (Mo$K\alpha$)	0.71073 Å	0.71073 Å
Crystal system, space group	Monoclinic, $P2_1/n$	Monoclinic, $P2_1/n$
a, b, c (Å)	7.8289(2), 14.5673(4), 6.7011(2)	7.8278(3), 14.5739(7), 6.6962(3)
β (°)	93.773(2)	93.820(4)
V (Å^3)	762.58(4)	762.22(6)
Z	4	4
μ (mm^{-1})	8.204	8.004
Crystal size (mm)	0.10 × 0.05 × 0.05	0.08 × 0.05 × 0.05
Θ-range for data collection (°)	2.80 to 40.87	3.35 to 32.15
Index ranges	$-14 \le h \le 14, -26 \le k \le 26, -12 \le l \le 12$	$-11 \le h \le 10, -21 \le k \le 21, -9 \le l \le 9$
Collected, independent and observed [$I > 2\sigma(I)$] reflections	48224, 4928, 3784	5213, 2452, 2027
R_{int}	0.068	0.036
Completeness to theta = 25.242°	100.0%	99.9%
Refinement		
Data / restraints / parameters	4928/2/129	2452/2/127
$R[F^2 > 2\sigma(F^2)]$, w$R(F^2)$, S	0.041, 0.092, 1.046	0.046, 0.078, 1.106
Extinction coefficient	0.0022(6)	0.0018(4)
$\Delta\varrho_{max}$, $\Delta\varrho_{min}$ (e Å^3)	1.390, −1.616	0.757, −0.896

Table 4 summarizes site occupancies, fractional atom coordinates and equivalent and isotropic displacement parameters. Crystallographic Information Files (CIF) are on deposit (see supplementary). From the interatomic distances listed in Table 5 and from a comparison of the two

average Mn-O distances, 2.181 and 2.186 Å, with the mean octahedral bond length reported in the literature for Mn^{2+}, one can preclude the presence of Mn in the trivalent oxidation state. The presence of V and As hosted in tetrahedra and the tetrahedrally coordinated site dimensions are in agreement with the pentavalent oxidation state for both cations, with *T*(1) slightly larger than *T*(2). The empirical bond valences estimated from the final refined structure (Table 6) also confirm the inferred cation oxidation states. The observed site scattering values obtained by structure refinement revealed that As^{5+} substitutes V^{5+} both at *T*(1) and *T*(2), but predominantly only at *T*(2) (Table 4), in agreement with a larger size for *T*(1).

Table 4. Site Occupancy Factor (s.o.f.), Atom Coordinates and Equivalent and Isotropic Displacement Parameters (Å^2) for Rüdlingerite Holotype from the Fianel Mine and Cotype from the Valletta Mine.

Site	s.o.f.	*x/a*	*y/b*	*z/c*	U_{eq}/U_{iso}*
Holotype					
Mn(1)	$Mn_{0.969(3)}$	0.4007(1)	0.3853(1)	0.2372(1)	0.014(1)
Mn(2)	$Mn_{0.969(3)}$	0.6240(1)	0.2483(1)	0.9594(1)	0.015(1)
T(1)	$V_{0.88(2)}As_{0.12(2)}$	0.3312(1)	0.4205(1)	0.7442(1)	0.012(1)
T(2)	$V_{0.26(3)}As_{0.74(3)}$	0.0426(1)	0.3170(1)	0.9482(1)	0.012(1)
O(1)	$O_{1.00}$	0.1693(2)	0.2927(1)	0.1566(3)	0.019(1)
O(2)	$O_{1.00}$	0.0609(2)	0.2350(1)	0.7722(3)	0.017(1)
O(3)	$O_{1.00}$	0.1208(2)	0.4185(1)	0.8441(3)	0.020(1)
O(4)	$O_{1.00}$	0.3859(3)	0.5277(1)	0.7039(3)	0.022(1)
O(5)	$O_{1.00}$	−0.1591(2)	0.3392(1)	-0.0024(3)	0.020(1)
O(6)	$O_{1.00}$	0.4627(3)	0.3688(1)	0.9229(3)	0.019(1)
O(7)	$O_{1.00}$	0.3177(3)	0.3586(1)	0.5294(3)	0.019(1)
OW(1)	$O_{1.00}$	0.2359(3)	0.5056(2)	0.2375(4)	0.030(1)
OW(2)	$O_{1.00}$	0.4048(3)	0.1509(2)	0.9400(4)	0.040(1)
H(1)	$H_{1.00}$	0.234(6)	0.554(2)	0.148(6)	0.036*
H(2)	$H_{1.00}$	0.354(6)	0.138(4)	0.811(4)	0.047*
Cotype					
Mn(1)	$Mn_{0.965}V^{3+}_{0.035}$	0.40146(8)	0.38561(5)	0.23771(10)	0.01235(18)
Mn(2)	$Mn_{0.965}V^{3+}_{0.035}$	0.62483(8)	0.24879(5)	0.95921(10)	0.01137(17)
T(1)	$V_{0.834(4)}As_{0.166(4)}$	0.33207(8)	0.42039(4)	0.74401(9)	0.00762(19)
T(2)	$V_{0.360(4)}As_{0.640(4)}$	0.04339(6)	0.31707(4)	0.94792(7)	0.00585(15)
O(1)	$O_{1.00}$	0.1697(4)	0.2924(2)	0.1562(4)	0.0158(6)
O(2)	$O_{1.00}$	0.0616(4)	0.2346(2)	0.7722(4)	0.0143(6)
O(3)	$O_{1.00}$	0.1224(4)	0.4184(2)	0.8441(5)	0.0170(6)
O(4)	$O_{1.00}$	0.3854(4)	0.5274(2)	0.7025(5)	0.0186(7)
O(5)	$O_{1.00}$	−0.1579(4)	0.3396(2)	-0.0038(5)	0.0177(7)
O(6)	$O_{1.00}$	0.4633(4)	0.3690(2)	0.9235(4)	0.0169(6)
O(7)	$O_{1.00}$	0.3184(4)	0.3584(2)	0.5304(4)	0.0165(6)
OW(1)	$O_{1.00}$	0.2351(4)	0.5051(2)	0.2393(6)	0.0265(8)
OW(2)	$O_{1.00}$	0.4060(5)	0.1513(3)	0.9401(6)	0.0354(10)
H(1)	$H_{1.00}$	0.201(7)	0.544(3)	0.134(6)	0.032*
H(2)	$H_{1.00}$	0.369(7)	0.093(2)	0.897(9)	0.042*

* Hydrogen atoms were refined using soft constraints and starting from the coordinates observed in the Fourier-difference maps; two further hydrogen atoms could not be located in the Fourier-difference map.

Table 5. Selected Interatomic Distances (Å) and Geometrical Parameters for the Rüdlingerite Fianel (Holotype) and Valletta (Cotype) Specimens.

		Holotype	**Cotype**			**Holotype**	**Cotype**
T(1)	–O(4)	1.647(2)	1.643(3)	*Mn*(1)	–O(4)	2.113(2)	2.113(3)
	–O(7)	1.696(2)	1.689(3)		–O(7)	2.139(2)	2.142(3)
	–O(6)	1.703(2)	1.702(3)		–O(2)	2.159(2)	2.158(3)
	–O(3)	1.818(2)	1.814(3)		–OW(1)	2.176(2)	2.175(3)
<*T*(1)	–O>	1.716	1.712		–O(6)	2.205(2)	2.204(3)
V	(Å^3)	2.585	2.567		–O(1)	2.295(2)	2.303(3)
Δ		0.02987	0.02978	<*Mn*(1)	–O>	2.181	2.182
T(2)	–O(5)	1.666(2)	1.662(3)	*Mn*(2)	–O(5)	2.155(2)	2.156(3)
	–O(1)	1.691(2)	1.694(3)		–O(6)	2.166(2)	2.164(3)
	–O(2)	1.696(2)	1.694(3)		–O(1)	2.167(2)	2.167(3)
	–O(3)	1.762(2)	1.761(3)		–O(2)	2.198(2)	2.199(3)
<*T*(2)	–O>	1.704	1.703		–O(7)	2.203(2)	2.206(3)
V	(Å^3)	2.529	2.525		–OW(2)	2.224(3)	2.223(4)
Δ		0.01696	0.01725	<*Mn*(2)	–O>	2.186	2.186
OW(1)	–*H*(1)	0.92(2)	0.93(2)	OW(2)	–*H*(2)	0.94(2)	0.94(2)
OW(1)	…O(5)	2.798(4)	2.801(5)	OW(2)	…O(5)	2.977(4)	2.984(6)
OW(1)	…O(4)	3.281(4)	3.259(6)	OW(2)	…O(1)	3.182(4)	3.178(6)
O(5) OW(1)	–O(4)	120.5(1)	120.4(1)	O(5)–OW(2)	–O(1)	111.0(1)	111.2(2)

Δ–distortion index defined after [28].

Table 6. Bond Valences (in Valence Units) for Rüdlingerite (Fianel Specimen) using [29].

	***Mn*(1)**	***Mn*(2)**	***T*(1)**	***T*(2)**	***H*(1)**	***H*(2)**	**Σ b.v.**
O(1)	0.26	0.36		1.26			1.88
O(2)	0.37	0.33		1.24			1.94
O(3)			0.94	1.03			1.97
O(4)	0.41		1.47				1.88
O(5)		0.37		1.35	0.06	0.10	1.88
O(6)	0.33	0.36	1.27				1.96
O(7)	0.38	0.33	1.29				2.00
OW(1)	0.35				1.00		1.35
OW(2)		0.31				0.95	1.26
SUM	2.10	2.06	4.97	4.88	1.06	1.058	

The polyhedral framework consists of octahedra and tetrahedra. The structural arrangement can be described in terms of edge-sharing octahedra forming zigzag chains subparallel to the [-101] direction. The chains of octahedra are decorated with T_2O_7 corner-connected dimmers (Figure 4a). The polyhedral framework contains cavities along [001] (Figure 4b). The cavities are elongated along [130] and [1-30]. The H_2O molecules are located on the unshared apexes of the octahedra that point towards these cavities (OW(1) and OW(2) sites), which form weak hydrogen bonds with neighboring O(5) atoms.

The crucial difference of the crystal structure of rüdlingerite with that of fianelite relates to the scattering at the *T*(2) site. Whereas the *T*(1) site has a scattering providing 24.20 electrons per site (eps), for the *T*(2) site, we refined 30.40 eps, which is consistent with a cation site occupancy strongly dominated by As^{5+}: $^{T(2)}(As_{0.74}V_{0.26})$ (Table 4). On the other hand, the *T*(1) site scattering, 24.20 eps, is consistent with a cation site occupancy dominated by V^{5+}: $^{T(1)}(V_{0.88}As_{0.12})$.

The refinement of intensity data collected on the cotype sample also yields a larger amount of scattering at the *T*(2) site (29.4(1) eps versus 24.7(1) eps at the *T*(1) site), also indicating the ordering of As at this site.

The mineral formula derived from the SREF information for the holotype and cotype samples are $Mn_{1.94}{}^{T(1)}(V^{5+}{}_{0.88}As_{0.12})^{T(2)}(As_{0.74}V^{5+}{}_{0.26})O_{7.00}\cdot 2H_2O$ and $Mn_2{}^{T(1)}(V^{5+}{}_{0.83}As_{0.17})^{T(2)}(As_{0.64}V^{5+}{}_{0.36})O_{7.00}\cdot 2H_2O$, respectively. These formulae show the dominance of V^{5+} at the *T*(1) site and As^{5+} at the *T*(2) site, and are consistent with the formulae derived from the chemical data (see above).

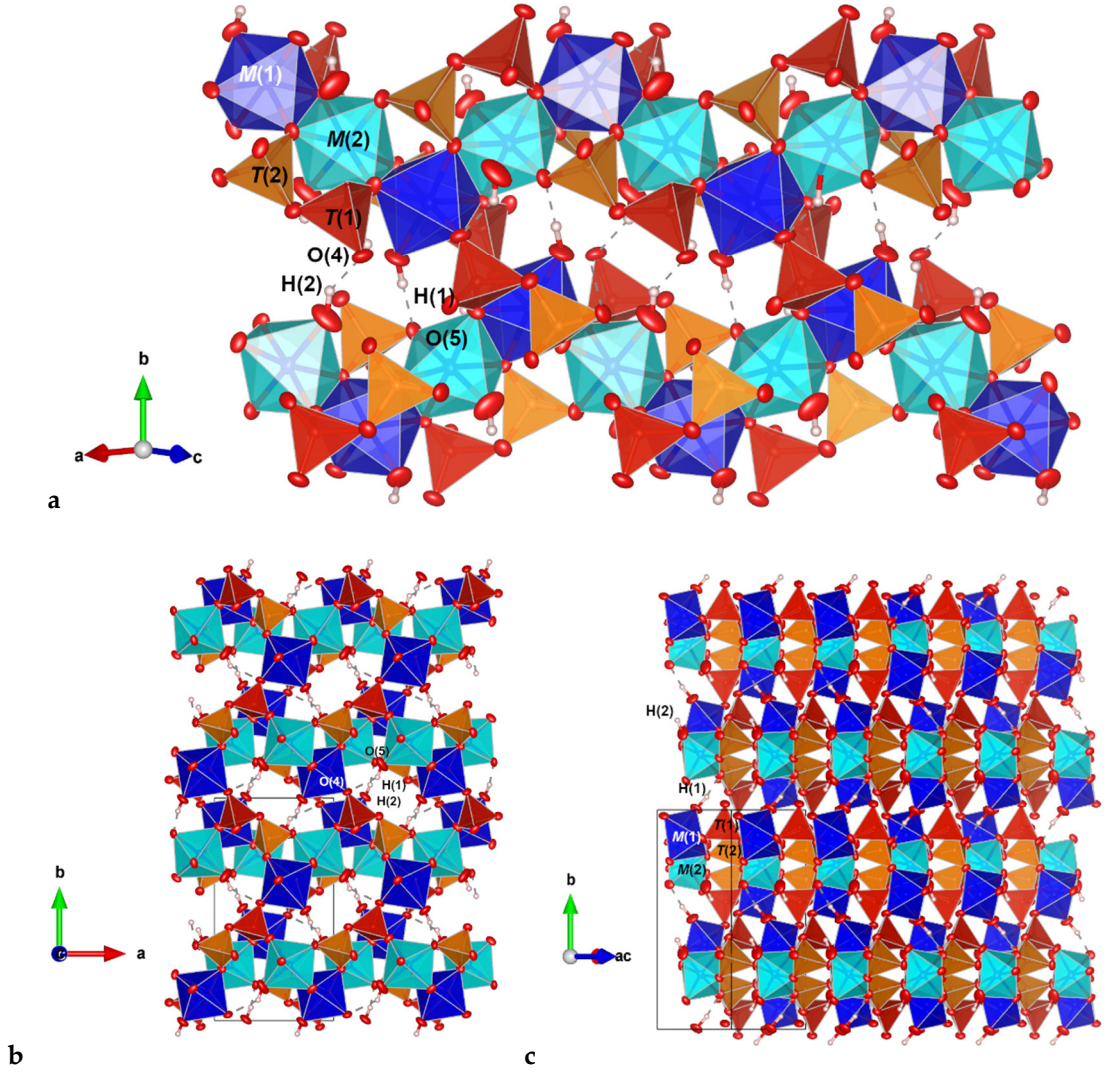

Figure 4. Orthographic projections of the crystal structure of rüdlingerite on the plain (the orientation is shown inside the figure), showing details of the chains of Mn-centred octahedra and the linking through the T_2O_7 groups (**a**), the cavities along [001] hosting the hydrogen bonds (**b**) and the alternance of bent chains along [010] (**c**). Oxygen atoms are reported in red as anisotropic displacement parameters. Hydrogen atoms are in white. Diagrams obtained using VESTA 3.0 [30].

7. Discussion

Rüdlingerite is the *T*(2) site As-dominant analogue of fianelite [1], with which it is isostructural. In their description of fianelite, Brugger and Berlepsch (1996) [1] reported an extended solid solution of As in fianelite (see Figure 5), which in fact reached more than 0.5 apfu of As in a couple of data points. However, the average of the chemical analyses yielded an amount of As which was lower than 0.5 apfu As. In fact, these authors described fianelite as $Mn_{1.98}(V_{1.57}As_{0.44}Si_{0.01})O_7\cdot 2H_2O$. Figure 5 shows the V-As homovalent substitution in rüdlingerite and fianelite, as derived from the available chemical analyses. However, all the structural data in fianelite and rüdlingerite show that As orders preferentially at the *T*(2) site (0.38 apfu in the model of Brugger and Berlepsch, 1996 [1]). Being *T*(1) and *T*(2) two crystallographically different sites, the dominance of an element on one of these sites

establishes a new mineral, in accord with the IMA-CNMNC rules. If As was ever found dominant in both the tetrahedral sites, that would represent a further new mineral species.

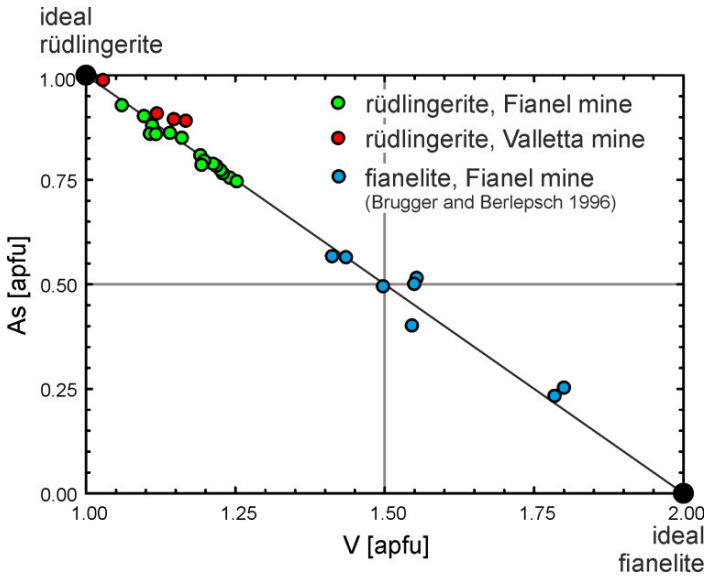

Figure 5. Distribution of As and V in rüdlingerite from the Fianel and Valletta mines and fianelite from the Fianel mine. Data of fianelite was redrawn from Brugger and Berlepsch (1996) [1].

There is a geometrical vantage to host a smaller cation at the *T*(2) sites: as can be seen in Figure 4, the chains of octahedra are bent, thus making it more propitious to have a smaller cation hosted at the *T*(2) tetrahedra at the concave hinge of the bent chain, while the *T*(1) tetrahedra acts as linkage of adjacent chains and therefore a larger size favours linkage. In fact, it is also more distorted (Table 5). This can explain the ability of fianelite/rüdlingerite structure to host both As and V, if available. The V^{5+}, on the other hand, is a d^0 transition metal and consequently prefers a more distorted bonding environment as the one observed in *T*(1) (Table 5).

Regarding hydrogen bonding, from Table 6, it is evident that the O(1) and O(4) have bond valence values clearly lower than 2, whereas the rest have values closer to 2 valence units (v.u.). This, along with the favourable geometries reported in Table 5, allow us to propose that the missing H atoms not located in the difference Fourier maps can form weak bonding to these oxygen atoms. Assuming a contribution equivalent to the one calculated for O(5) (Table 6) would be enough to reach a bond valence sum of 2 v.u. The bond valence sum values lower than 2 at OW(1) and OW(2) indicate the respective bonds to the two missing H atoms, probably longer than the ones observed during refinement for H(1) and H(2). It is worth noting that the O(3) atom, proposed by Brugger and Berlepsch (1996) as acceptor of H-bonding, does not seem a probable acceptor as the bond valence incidence is about 2 v.u. Accounting for the above scheme, it is possible to use the empirical correlation of Libowitzky [31] to calculate the frequency of the corresponding O–H using the observed $O_D \cdots O_A$ lengths (Table 5) for the four proposed hydrogen bonds. We obtain 3400, 3542, 3581, and 3587 cm^{-1}, which are in line with the bands observed in the Raman of the sample from Fianel (Figure 3).

Mesaite [32], ideally $CaMn^{2+}{}_5(V_2O_7)_3 \cdot 12H_2O$, is structurally related to the above two mineral species, having the same zig-zag chains of Mn^{2+} centred octahedra and divanadate tetrahedra groups as fianelite and rüdlingerite. However, it has a layer structure, with interlayers regions having solvated Ca cations, whereas fianelite and rüdlingerite have a framework structure. Comparisons of physical data of rüdlingerite, fianelite, and mesaite are summarized in Table 7.

Table 7. Comparison of Rüdlingerite, Fianelite, and Mesaite.

Mineral	Rüdlingerite [This Work] (Fianel/Valletta)	Fianelite [1]	Mesaite [32]
Simplified formula	$Mn^{2+}_2V^{5+}As^{5+}O_7{\cdot}2H_2O$	$Mn^{2+}_2V^{5+}_2O_7{\cdot}2H_2O$	$CaMn^{2+}_5(V_2O_7)_3{\cdot}12H_2O$
Space group	$P2_1/n$	$P2_1/n$	$P2/n$
a (Å)	7.8289(2)/7.8278(3)	7.809(2)	9.146(2)
b (Å)	14.5673(4)/14.5739(7)	14.554(4)	10.424(3)
c (Å)	6.7011(2)/6.6962(3)	6.705(4)	15.532(4)
β (°)	93.773(2)/93.820(4)	93.27(3)	102.653(7)
V (Å^3)	762.58(4)/762.22(6)	760.8(5)	1444.8(6)
Z	4	4	2
$D_{calc.}$ (g/cm^3)	3.298/3.322	3.217	2.744
$D_{meas.}$ (g/cm^3)		3.21(1)	2.74(1)
Strongest reflections in the X-ray powder diffraction data, d/n (Å) (I)	3.048(100)	3.039(100)	10.47(100)
	5.34(80)	5.32(80)	2.881(25)
	2.730(60)	2.721(60)	3.568(24)
	2.206(60)	1.593(60)	3.067(17)
	2.344(50)	3.436(50)	4.30(11)
	7.28(50)	3.259(50)	2.615(11)
	6.88(30)	2.573(50)	8.60(10)
Optical class, sign	Biaxial; sign unknown	unknown	biaxial (–)
α (589.3 nm)	n_{av} =1.791 − 1.799 (calc.)		1.760 (calc.)
β		1.82(2)	1.780(5)
γ			1.795(5)
$2V_{meas}$ (°)	<10°	<10°	81(2)°
$2V_{calc}$ (°)			unknown

In the Strunz system [33], rüdlingerite belongs to 8.FC: polyphosphates, polyarsenates, and polyvanadates with H_2O.

Arsenates and vanadates are known to occur in numerous, metamorphosed Fe-Mn deposits that underwent multiphase Alpine metamorphism all across the Alps and the Apennines. The paleogeographic environment of these mineralizations are diverse, with some deposits being hosted in Jurassic-aged radiolarites like Falotta, Grisons, Switzerland [34] or Val Graveglia, Liguria, Italy [35], another occurring in platform-carbonates sedimented over a continental basement like Fianel or in Middle Jurassic-aged paleokarsts filling with hydrothermal input like Pipjigletscher, Valais, Switzerland [36], and yet other being hosted in Permian quartzites like Valletta. These vanadium-arsenic-manganese-minerals Alpine parageneses have formed partly during prograde metamorphism, up to upper greenschist-facies conditions culminating at about 450° C at pressures of 4 to 6 kbar in Pipjigletscher [36] and – like rüdlingerite – partly though hydrothermal processes during retrograde metamorphism [37]. Strangely, the Prabornaz Mn-deposit, Aosta, Italy, also of sedimentary-hydrothermal origin but affected by a high metamorphism at about 550° C at pressure of 21 kbar, is almost devoid of V and weakly enriched in As [38,39].

Rüdlingerite is the twenty-fifth new Mn vanadate or arsenate to be described from such Fe-Mn Alpine deposits. While their mineralogy is highly contrasted and fascinating, their economic significance was very modest, due to their small volumes, pronounced compartmentalization and/or difficult, high-altitude access. This strongly contrasts with the other large providers of Mn arsenates and vanadates deposits that are not linked to an Alpine event: Långban, Sweden, Franklin, and Sterling Hill, USA as well as Kombat, Namibia.

Supplementary Materials: The following are available online at www.mdpi.com/xxx, Crystallographic Information Files: ruedlingerite_Fianel.cif and ruedlingerite_Valletta.cif.

Author Contributions: Recognition of first rüdlingerite samples, P.R., R.B., and M.E.C.; preliminary analysis, P.R., N.M., and M.E.C.; physical measurements, R.S., F.C., and U.H.; Raman spectroscopic measurements, C.S. and M.E.C.; crystal-structure solution and refinement, F.N., F.C., and F.B.; chemical analyses, R.S., F.N., and F.B.; writing—proposal for IMA; N.M. with contributions from all authors; writing—original draft preparation, P.R. with contributions from all authors; writing—review and editing, P.R., F.C. with contributions from all authors. All authors have read and agreed to the published version of the manuscript.

Funding: The Article Processing Charge for this article was supported by Etat de Vaud through Musée cantonal de géologie in Lausanne, Switzerland.

Acknowledgments: This work would not have been possible without the enthusiasm of M. Francesco Vanini (Varese, I), who brought his "fianelite" discovery to the attention of one of us (P.R.), allowed us to link the two teams, and subsequently supported our study with his field experience. We thank Cristian Biagioni for the constructive and fruitful discussions. The review by Mark Cooper and other three anonymous referees greatly enhanced the manuscript.

Conflicts of Interest: The authors declare no conflict of interest.

References

1. Brugger, J.; Berlepsch, P. Description and crystal structure of fianelite, $Mn_2V(V,As)O_7{\cdot}2H_2O$, a new mineral from Fianel, Val Ferrera, Graubünden, Switzerland. *Amer. Mineral.* **1996**, *81*, 1270–1276. https://doi.org/10.2138/am-1996-9-1025.
2. Stucky, K. Die Eisen- und Maganerze in der Trias des Val Ferrera. *Beitr. Geol. Schweiz, Geotechn. Ser*. **1960**, *37*, 60.
3. Brugger, J.; Berlepsch, P.; Meisser, N.; Armbruster, T. Ansermetite, $MnV_2O_6{\cdot}4H_2O$, a new mineral species with V^{5+} in five-fold coordination from Val Ferrera, Eastern Swiss Alps. *Can. Mineral.* **2003**, *41*, 1423–1431. https://doi.org/10.2113/gscanmin.41.6.1423.
4. Brugger, J.; Krivovichev, S.; Meisser, N.; Ansermet, S.; Armbruster, T. Scheuchzerite, $Na(Mn,Mg)_9[VSi_9O_{28}(OH)](OH)_3$, a new single-chain silicate. *Amer. Mineral.* **2006**, *91*, 937–943. https://doi.org/10.2138/am.2006.1965.
5. Nickel, E.H.; Grice, J.D. The IMA Commission on New Minerals and Mineral Names: Procedures and guidelines on mineral nomenclature. *Can. Mineral.* **1998**, *36*, 913–926.
6. Hatert, F.; Burke, E.A.J. The IMA-CNMNC dominant-constituent rule revisited and extended. *Can. Mineral.* **2008**, *46*, 717–728.
7. Bosi, F.; Hatert, F.; Hålenius, U.; Pasero, M.; Miyawaki, R.; Mills, S.J. On the application of the IMA-CNMNC dominant-valency rule to complex mineral compositions. *Mineral. Mag.* **2019**, *83*, 627–632. https://doi.org/10.1180/mgm.2019.55.
8. Roth, P. ; Meisser, N. Rüdlingerite, une nouvelle espèce minérale de Fianel (GR). *Cristallier Suisse*, **2018**, *52*, 26–29.
9. Schmid, S.M.; Rück, P.; Schreurs, G. The significance of the Schams nappes for the reconstruction of the paleotectonic and orogenic evolution of the Penninic zone along the NFP-20 East traverse (Grisons, Eastern Switzerland). *Mém. Soc. Géol. France*, **1990**, *156*, 263–287.
10. Cámara, F.; Ciriotti, M.E.; Bittarello, E.; Nestola, F.; Massimi, F.; Radica, F.; Costa, E.; Benna, P.; Piccoli, G.C. Arsenic-bearing new mineral species from Valletta mine, Maira Valley, Piedmont, Italy: I. Grandaite, $Sr_2Al(AsO_4)_2(OH)$, description and crystal structure. *Mineral. Mag.* **2014**, *78*, 757–774. https://doi.org/10.1180/minmag.2014.078.3.21.
11. Cámara, F.; Bittarello, E.; Ciriotti, M.E.; Nestola, F.; Radica, F.; Marchesini, M. As-bearing new mineral species from Valletta mine, Maira Valley, Piedmont, Italy: II. Braccoite, $NaMn^{2+}{}_5[Si_5AsO_{17}(OH)](OH)$, description and crystal structure. *Mineral. Mag.* **2015**, *79*, 171–189. https://doi.org/10.1180/minmag.2014.078.3.21.
12. Cámara, F.; Bittarello, E.; Ciriotti, M.E.; Nestola, F.; Radica, F.; Massimi, F.; Balestra, C.; Bracco, R. As-bearing new mineral species from Valletta mine, Maira Valley, Piedmont, Italy: III. Canosioite, $Ba_2Fe^{3+}(AsO_4)_2(OH)$, description and crystal structure. *Mineral. Mag.* **2017**, *81*, 305–317. https://doi.org/10.1180/minmag.2016.080.097.
13. Kampf, A.R.; Cámara, F.; Ciriotti, M.E.; Nash, B.P.; Balestra, C.; Chiappino, L. Castellaroite, $Mn_2^{+3}(AsO_4)_2{\cdot}4{\cdot}5H_2O$, a new mineral from Italy related to metaswitzerite. *Eur. J. Mineral.* **2016**, *28*, 687–696. 10.1127/ejm/2016/0028-2535.
14. Cámara, F.; Bosi, F.; Ciriotti, M.E.; Bittarello, E.; Hålenius, U.; Balestra, C. Lombardoite, IMA 2016-058. CNMNC Newsletter No. 33. *Mineral. Mag.* **2016**, *80*, 1135–1144.
15. Cámara, F.; Biagioni, C.; Ciriotti, M.E.; Bosi, F.; Kolitsch, U.; Paar, W.H.; Blass, G.; Bittarello, E. Piccoliite, IMA2017-016. CNMNC Newsletter No. 37. *Mineral. Mag.* **2017**, *81*, 737–742.
16. Meyrowitz, R. A compilation and classification of immersion media of high index of refraction. *Amer. Mineral.* **1955**, *40*, 398–409.
17. Jelley, E.E. A microrefractometer and its use in chemical microscopy. *J. Royal Microsc. Soc., London*, **1934**, *54*, 234–245.

18. Merlet, C. An Accurate Computer Correction Program for Quantitative Electron Probe Microanalysis. *Microchim. Acta*, **1994**, *114/115*, 363–376.
19. *LabSpec*, Version 5.64.15; Software for Raman Spectroscopic Data Analysis, Acquisition and Manipulation; HORIBA Jobin Yvon SAS: Villeneuve d'Ascq, France, 2005
20. Wojdyr, M. Fityk: A general-purpose peak fitting program. *J. Appl. Crystallogr.* **2010**, *43*, 1126–1128. https://doi.org/10.1107/S0021889810030499.
21. Adams, D.M.; Gardner, I.R. Single-crystal vibrational spectra of apatite, vanadinite, and mimetite. *J. Chem. Soc., Dalton Trans.* **1974**, *14*, 1505–1509.
22. Frost, R.L.; Sejkora, J.; Cejka, J.; Keefe, E.C. Vibrational spectroscopic study of the arsenate mineral strashimirite $Cu_8(AsO_4)_4(OH)_4.5H_2O$ – Relationship to other basic copper arsenates. *Vibr. Spectrosc.* **2009**, *50*, 289–297. https://doi.org/10.1016/j.vibspec.2009.02.002.
23. Nakamoto, K. *Infrared and Raman Spectra of Inorganic and Coordination Compounds*. Wiley: New York, NY, USA, 1986; p. 432.
24. Farmer, V.C. *The Infrared Spectra of Minerals*. Mineralogical Society: London, UK, 1974; p. 539.
25. Myneni, S.C.B.; Traina, S.J.; Waychunas, G.A.; Logan, T.J. Experimental and Theoretical Vibrational Spectroscopic Evaluation of Arsenate coordination in Aqueous solutions and Solids. *Geochim. Cosmochim. Acta*, **1998**, *62*, 3285–3300. https://doi.org/10.1016/S0016-7037(98)00222-1.
26. Schwarzenbach, D.; King, G. *LATCON in Xtal3.6*; Hall, S. R., du Boulay, D.J. & Olthof-Hazekamp, R., Eds; University of Western Australia: Perth, Australia, 1999.
27. Sheldrick, G.M. A short history of SHELX. *Acta Crystallograph.* **2008**, *A64*, 112–122. https://doi.org/10.1107/S0108767307043930.
28. Baur, W.H. The geometry of polyhedral distortions. Predictive relationships for the phosphate group. *Acta Crystallograph.* **1974**, *B30*, 1195–1215.
29. Gagné, O.C.; Hawthorne, F.C. Comprehensive derivation of bond-valence parameters for ion pairs involving oxygen. *Acta Crystallograph.* **2015**, *B71*, 562–578. https://doi.org/10.1107/S2052520615016297
30. Momma, K.; Izumi, F. VESTA 3 for three-dimensional visualization of crystal, volumetric and morphology data. *J. Appl. Crystallogr.* **2011**, *44*, 1272–1276.
31. Libowitzky, E. Correlation of O–H stretching frequencies and O–H···O hydrogen bond lengths in minerals. *Monatshefte für Chemie*, **1999**, *130*, 1047–1059.
32. Kampf, A.R.; Nash, B.P.; Marty, J.; Hughes, J.M. Mesaite, $CaMn^{2+}_5(V_2O_7)_3{\cdot}12H_2O$, a new vanadate mineral from the Packrat mine, near Gateway, Mesa County, Colorado, USA. *Mineral. Mag.* **2017**, *81*, 319–327.
33. Strunz, H. ; Nickel, E.H. *Strunz Mineralogical Tables. Chemical Structural Mineral Classification System*, 9th ed; E. Schweizerbart, Stuttgart, Germany, 2001; p. 870.
34. Geiger, T. Manganerze in den Radiolariten Graubündens. *Beitr. Geol. Schweiz*, **1948**, *27*, 85. http://e-collection.library.ethz.ch/eserv/eth:21226/eth-21226-01.pdf.
35. Cortesogno, L.; Lucchetti, G.; Penco, A.M. Le mineralizzazioni a manganese nei diaspri delle ofioliti liguri: Mineralogie e genesi. *Rendiconti Soc. Ital. Mineral. Petrol.* **1979**, *35*, 151–197.
36. Brugger, J.; Meisser, N. Manganese-rich assemblages in the Barrhorn Unit, Turtmanntal, Central Alps, Switzerland. *Can. Mineral.* **2006**, *44*, 229–248. https://doi.org/10.2113/gscanmin.44.1.229.
37. Brugger, J.; Gieré, R. As, Sb, Be and Ce enrichment in minerals from a metamorphosed Fe-Mn deposit, Val Ferrera, eastern Swiss Alps. *Can. Mineral.* **1999**, *37*, 37–52.
38. Tumiati, S.; Martin, S.; Godard, G. Hydrothermal origin of manganese in the high- pressure ophiolite metasediments of Praborna ore deposit (Aosta Valley, Western Alps). *Eur. J. Mineral.* **2010**, *22*, 577–594. https://dx.doi.org/10.1127/0935-1221/2010/0022-2035.
39. Tumiati, S.; Merlini, M.; Godard, G.; Hanfland, M.; Fumagalli, P. Orthovanadate wakefieldite-(Ce) in symplectites replacing vanadium-bearing omphacite in the ultra-oxidized manganese deposit of Praborna (Aosta Valley, Western Italian Alps). *Amer. Mineral.* **2020**, *105*, 1242–1253. https://doi.org/10.2138/am-2020-7219.